JOURNAL OF AIRCRAFT
Vol. 42, No. 5, September–October 2005

Biodynamic Response Mitigation to Shock Loads Using Magnetorheological Helicopter Crew Seat Suspensions

Young-Tai Choi* and Norman M. Wereley†
University of Maryland, College Park, Maryland 20742

Biodynamic response mitigation of both sinusoidal vibration and shock loads using a magnetorheological (MR) seat suspension is investigated. In doing so, an MR seat suspension model for helicopters, with a detailed lumped parameter model of a human body, was developed. The lumped parameter model of the human body consists of four parts: pelvis, upper torso, viscera, and head. From the model, the governing equation of motion of the MR seat suspension considering the human body was derived. Based on this equation, a semi-active nonlinear optimal control algorithm appropriate for the MR seat suspension was developed. The simulated control performance of the MR seat suspension was evaluated under both sinusoidal vibration and shock loads due to a vertical crash landing of a helicopter. In addition, the mitigation of injuries to humans due to such shock loads was also evaluated and compared with that of the passive seat suspension using a passive hydraulic damper.

Introduction

RECENTLY, the minimization of shock load-induced injury has become a critical issue in helicopter seat suspension design. In most cases, pilot or occupant spinal and pelvic injuries result from a harsh vertical landing or crash landing. However, the severity of this injury can be considerably minimized if the helicopters are equipped with crashworthy seat designs.[1,2] A seat suspension can be used to mitigate shock loads that are transmitted from the base frame of the aircraft and helicopter and transmitted to the human body.

There are three potential seat suspensions designs: passive, semi-active, and active. A major drawback of a passive seat suspension based on viscoelastic or hydraulic means is that it has limited performance because damping or stiffness is not controllable.[3] Many researchers have been inspired to develop novel seat suspensions showing improved shock and vibration attenuation performance by permitting stiffness or damping to be adaptable or controllable.

Improved shock and vibration attenuation performance can be achieved through semi-active or active seat suspensions. Active seat suspensions featuring electromagnetic, electropneumatic, and servovalves can provide high shock attenuation performance over a wide frequency range.[4] However, active seat suspensions require high power, complex configurations, and sophisticated control algorithms. Recently, to mitigate these drawbacks associated with active seat suspensions, semi-active seat suspensions have been introduced. The semi-active seat suspension combines the best features of passive and active seat suspensions. Like passive seat suspensions, the semi-active seat suspension develops control forces in response to seat and other motions. Therefore, even in the case of actuator failure, the semi-active seat suspensions can still suppress shock using the passive damping characteristics of the suspension. In addition, control forces of semi-active seat suspensions can be adjusted via control algorithms, just as in active seat suspensions, but with substantially reduced power requirements.

There are several semi-active actuator candidates based on devices such as rotary solenoid, stepper motor, and electrorheological (ER)/magnetorheological (MR) valves. Among these, a very attractive candidate for effective semi-active seat suspensions is to use MR fluid-based damping devices. MR fluids are suspension of soft magnetic powder, that is, low-coercivity powders such as pure iron or cobalt, in hydraulic or silicone carrier oil. Under the application of magnetic field, the particles form chains and the fluid resists flow in the presence of a pressure gradient, as might be seen in the valve of a damper. This leads to the capability of controllable conditions including change of natural frequency (as when the payload or crew member weight changes), shock load (magnitude and duration), and vibration load (amplitude and frequency). The key physical effect is that the application of magnetic field causes the powder in the MR fluid to form chains, which is manifested in an appreciable yield stress of the MR fluid. [As high as 70 kPa has been measured by Lord Cooperation (http://www.rheonetic.com/fluid_begin.htm).] These MR fluids can rapidly adjust their rheological properties in response to external fields. As a result, seat suspensions utilizing dampers with MR valves have features such as continuously controlled damper force and fast response times, typically 10 ms (Ref. 5).

Wu and Griffin[6] reviewed several semi-active control algorithms and proposed a new semi-active on–off control policy to reduce the severity of seat suspension end-stop impacts. They used an ER seat damper to realize the control policy. It was found that the on–off control policy was successful when implemented into the ER seat suspension in improving vibration isolation performance and reducing end-stop impact. Choi et al.[7] constructed a two-degree-of-freedom ER seat suspension for a commercial vehicle and experimentally evaluated the attenuation of seat vibration under a sliding mode controller. In addition, they theoretically configured a full-car model consisting of primary, cabin, and seat suspensions, and its vibration isolation performance was evaluated by the hardware-in-the-loop simulation method. They also developed an MR seat suspension for a large-size commercial truck and evaluated its vibration control performance under a simple skyhook control algorithm.[8] Park and Jeon[9] proposed a Lyapunov-based robust control algorithm that can compensate for disadvantages due to the time delay of actuators and evaluated vibration control performance of one-degree-of-freedom MR seat suspension under the Lyapunov-type robust control algorithm. McManus et al.[10] investigated the benefits of an MR seat suspension in reducing the incidence and severity of end-stop impacts. They showed the MR seat suspension has superior end-stop impact attenuation performance and reduces vibration exposure levels.

Most research on ER/MR seat suspensions has evaluated responses of the seat suspension itself caused by road-induced shock and vibration. However, studies on the effect of the shock and vibration on seated personnel are much less explored. Therefore, the main goal of this study is to analyze the biodynamic response of the

Presented as Paper AHS 2003-280 at the 59th Annual Forum of the American Helicopter Society, Phoenix, AZ, 6–8 May 2003; received 3 December 2003; revision received 8 October 2004; accepted for publication 8 December 2004.

*Assistant Research Scientist, Smart Structures Laboratory, Alfred Gessow Rotorcraft Center, Department of Aerospace Engineering.

†Professor, Smart Structures Laboratory, Alfred Gessow Rotorcraft Center, Department of Aerospace Engineering. Associate Fellow AIAA.

human body protected by MR seat suspensions to both sinusoidal vibration and shock loads and to compare these results with a passive hydraulic seat suspension. In doing so, an MR seat suspension model for helicopters was developed with the following features: 1) a detailed nonlinear MR damper model considering hysteresis loop in damper force vs piston velocity, 2) a detailed lumped parameter model of the human body, 3) shock responses appropriate to high sink rate levels of 6.1–12.2 m/s (20–40 ft/s). The lumped parameter model of the human body consists of four parts: pelvis, upper torso, viscera, and head. From the model, the governing equation of motion of the MR seat suspension considering the human body was derived. Based on this equation, a semi-active nonlinear optimal control algorithm appropriate for the MR seat suspension was developed. The simulated biodynamic responses of the MR seat suspension was evaluated under both sinusoidal vibration and shock loads due to a vertical crash landing of a helicopter. In addition, the mitigation of injuries to crew due to such shock loads was also evaluated and compared with that of the passive hydraulic seat suspension.

MR Seat Suspensions

A helicopter crew seat model that includes an MR seat suspension and seated personnel for a vertical high sink rate landing of a helicopter can be described by using the lumped parameter model as shown in Fig. 1. The seat denoted by M_1 is fixed to the floor through the MR seat suspension that consists of an MR damper and a coil spring and is modeled by spring K_1, damping C_1, and yield force F_y. In addition, the end-stop buffer that produces the reaction force when suspension stroke exceeds its free-suspension travel is installed at the floor and simply modeled by nonlinear spring reaction force F_{st}. The soft seat cushion is configured on the seat and, because its mass is small, its mechanical model is simply represented by spring K_{2c} and damping C_{2c}. In this study, the human sits upright on the seat cushion on the seat and consists of four parts: pelvis, upper torso, viscera, and head. Four parts of the human body are modeled by nonlinear lumped parameter systems comprising mass M_i, spring K_i, and damping C_i for $i = 2, 3, 4$, and 5. Here z_i, $i = 2, 3, 4, 5$, coordinates are the displacement of the human body for pelvis, upper torso, viscera, and head, respectively. Note that when a human body sits on a seat, only 71% of the total weight is supported by the seat, and the remaining body weight is supported by the feet.[11] Therefore, in this human body model, the pelvis includes the femur, but excludes the lower legs and feet. In addition, z_0 and $\dot{z}_0$ are the displacement and velocity of the floor excitation due to a crash impact.

During a harsh or crash landing, the floor of the helicopter undergoes a shock deceleration. This shock deceleration is transmitted to the human body through the MR seat suspension. At this point, if the MR seat suspension mitigates the shock transmitted to the human body properly, injury of seated personnel will decrease.

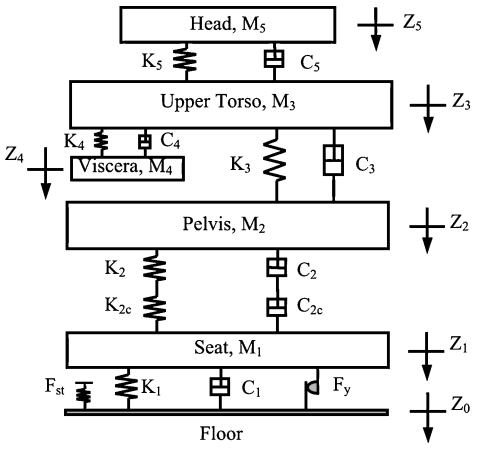

Fig. 1 Mechanical model for MR helicopter crew seat suspension coupled with human body.

The motion of the MR seat suspension is governed by

$$M_1\ddot{z}_1 = -K_1(z_1 - z_0) - C_1(\dot{z}_1 - \dot{z}_0) + K_{2t}(z_2 - z_1) + C_{2t}(\dot{z}_2 - \dot{z}_1) - F_y \tag{1}$$

$$M_2\ddot{z}_2 = -K_{2t}(z_2 - z_1) - C_{2t}(\dot{z}_2 - \dot{z}_1) + K_3(z_3 - z_2) + C_3(\dot{z}_3 - \dot{z}_2) \tag{2}$$

$$M_3\ddot{z}_3 = -K_3(z_3 - z_2) - C_3(\dot{z}_3 - \dot{z}_2) - K_4(z_3 - z_4) - C_4(\dot{z}_3 - \dot{z}_4) + K_5(z_5 - z_3) + C_5(\dot{z}_5 - \dot{z}_3) \tag{3}$$

$$M_4\ddot{z}_4 = K_4(z_3 - z_4) + C_4(\dot{z}_3 - \dot{z}_4) \tag{4}$$

$$M_5\ddot{z}_5 = -K_5(z_5 - z_3) - C_5(\dot{z}_5 - \dot{z}_3) \tag{5}$$

with initial conditions

$$z_0 = z_1 = z_2 = z_3 = z_4 = z_5 = 0$$

$$\dot{z}_0 = \dot{z}_1 = \dot{z}_2 = \dot{z}_3 = \dot{z}_4 = \dot{z}_5 = v_0 \tag{6}$$

where

$$K_{2t} = \frac{K_2 K_{2c}}{K_2 + K_{2c}}, \qquad C_{2t} = \frac{C_2 C_{2c}}{C_2 + C_{2c}} \tag{7}$$

Here, v_0 is the initial vertical landing velocity of the helicopter. It is assumed that the deceleration applied to the floor due to a high sink rate landing is in the form of a half-sine function with a short duration and is defined as[12,13]

$$\ddot{z}_0 = \begin{cases} -(\pi v_0/2t_s)\sin(\pi t/t_s), & \text{if} \quad 0 \le t \le t_s \\ 0, & \text{if} \quad t > t_s \end{cases} \tag{8}$$

where t_s is the shock duration. The spring coefficient of the pelvis, K_2, is characterized by the nonlinear function[14]

$$K_2 = \begin{cases} 1.6215e8(z_2 - z_1)^2, & \text{if} \quad (z_2 - z_1) \ge 0 \\ 0, & \text{if} \quad (z_2 - z_1) < 0 \end{cases} \tag{9}$$

The spring coefficient of the upper torso is also [14]

$$K_3 = \begin{cases} 3.78e6 + 1.09e7(z_2 - z_3) - 2.69e7(z_2 - z_3)^2, & \text{if} \quad (z_2 - z_3) \ge 0.04 \\ 77044, & \text{if} \quad (z_2 - z_3) < 0.04 \end{cases} \tag{10}$$

The damping coefficient C_i is given by

$$C_i = 2\zeta_i\sqrt{M_i K_i}, \qquad \text{if} \quad i = 2, 3, 4, 5 \tag{11}$$

where ζ_i is the damping ratio of each part of the human body and can be identified by dynamic tensile test.[14] Note that because K_2 and K_3 are nonlinear functions, C_2 and C_3 are also nonlinear functions. The parameters of the MR seat suspension model are specified in Table 1. The yield force F_y due to yield stress of MR fluids is characterized by a nonlinear hysteresis model and is expressed by[15]

$$F_y = F_0 \tanh\{[(\dot{z}_1 - \dot{z}_0) + \lambda_1(z_1 - z_0)]\lambda_2\} \tag{12}$$

where F_0 is the magnitude of the yield force and can be continuously adjusted by applied magnetic field strength. Here λ_1 and λ_2 are characteristic parameters of the nonlinear hysteresis model to capture the hysteresis loop in damper force vs piston velocity. In this study, $\lambda_1 = 7.5$ and $\lambda_2 = 65$ are assumed to be constant. Typical damping force behavior of the nonlinear hysteresis model given by Eq. (12) is shown in Fig. 2. In Fig. 2, the damping force vs piston velocity plot obtained from the model has a hysteresis cycle in the low-velocity region, similar to a practical case.[15] In addition, the nonlinear hysteresis model shows that, as the strength of the applied field increases, the damping force also increases.

Table 1 Parameters of the MR seat suspension model

Quantity	Symbol	Value	Units
Mass of seat	M_1	13.5	kg
Mass of pelvis	M_2	29	kg
Mass of upper torso	M_3	21.8	kg
Mass of viscera	M_4	6.8	kg
Mass of head	M_5	5.5	kg
Stiffness of coil spring	K_1	22.6	kN/m
Stiffness of soft seat cushion	K_{2c}	37.7	kN/m
Stiffness of viscera	K_4	2.84	kN/m
Stiffness of head	K_5	202.3	kN/m
Damping of MR damper due to viscous component	C_1	750	N · s/m
Damping of soft seat cushion	C_{2c}	159	N · s/m
Damping ratio of pelvis	ζ_2	0.25	——
Damping ratio of upper torso	ζ_3	0.11	——
Damping ratio of viscera	ζ_4	0.5	——
Damping ratio of head	ζ_5	0.1	——

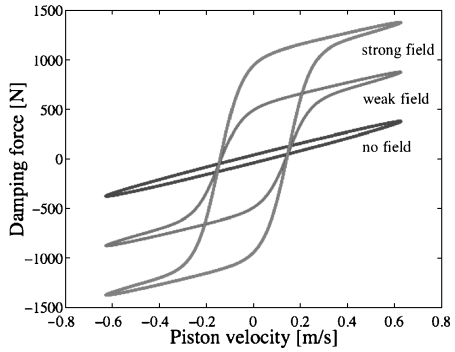

Fig. 2 Typical damping force behavior of hysteresis model in force vs piston velocity.

On the other hand, when the suspension stroke exceeds its free-suspension travel z_{st}, the end-stop buffer produces the nonlinear spring reaction force F_{st} given by[16]

$$F_{st} = 1.2e6[z_1 - z_0 - z_{st}\,\mathrm{sgn}(z_1 - z_0)] + 5.1e9[z_1 - z_0 - z_{st}\,\mathrm{sgn}(z_1 - z_0)]^3 \tag{13}$$

to prevent metal-to-metal contact. In this study, because the vertical free space from the floor to the seat in a helicopter is within about 343 mm (13.5 in.) (Ref. 17), the full stroke of the MR seat suspension is chosen to be 101.6 mm (4 in.), and its free-suspension travel z_{st} is 88.9 mm (3.5 in). In addition, the end-stop buffer is assumed to be installed at the floor. Note that a long-stroke MR seat suspension is possible, but it may require very complex mechanisms so that the helicopter pilot maintains control of pedals and the unwanted friction force of the damper increases. In general, the full stroke of seat dampers for freight and resource sector vehicles is designed to provide free travel ranging from 100 to 150 mm (Ref. 10). Based on this, the free-suspension travel of 88.9 mm is a reasonable value and would be easy to implement. In addition, note that, in the process of calculating the response of the MR seat suspension, the static load $-F_{st}$ is added to the right-hand side of Eq. (1) when $|z_1 - z_0| > z_{st}$.

Nonlinear Optimal Control for MR Seat Suspensions

To mitigate the sinusoidal vibration and crashing shock loads of the helicopter using a MR seat suspension, a nonlinear optimal control is adopted. To decrease the order of the nonlinear optimal controller, we reduce the MR seat suspension model considering the human body given by Eqs. (1–5). Because z_2, z_3, z_4, and z_5 describe the displacement of each part of the human body, these are not measurable or observable in a practical sense. In addition, because the shock load of the seat is directly transmitted to the human body, we can expect that, if the shock load at the seat decreases, the shock at each part of the human body would also decrease by intuition. Therefore, the dynamics of the human body is neglected in the process of nonlinear control design by considering it as a rigid body. In a practical sense, actuation forces cannot be applied directly to the human body, only restraint forces.

Now, the reduced MR seat suspension model can be rewritten in the form of the state-space model with states $x = [x_1 \;\; x_2]^T = [z_1 \;\; \dot{z}_1]^T$, input $u = F_0$, and disturbances $w = [w_1 \;\; w_2]^T = [z_0 \;\; \dot{z}_0]^T$, that is,

$$\dot{x} = f(x) + g(x, w)u + \sum_{k=1}^{2} d_k w_k \tag{14}$$

where

$$f(x) = \begin{bmatrix} x_2 \\ -\dfrac{K_1}{M}x_1 - \dfrac{C_1}{M}x_2 \end{bmatrix} \tag{15}$$

$$g(x, w) = \begin{bmatrix} 0 \\ -\dfrac{\tanh\{[(x_2 - w_2) + \lambda_1(x_1 - w_1)]\lambda_2\}}{M} \end{bmatrix} \tag{16}$$

$$d_1 = \begin{bmatrix} 0 \\ \dfrac{K_1}{M} \end{bmatrix}, \qquad d_2 = \begin{bmatrix} 0 \\ \dfrac{C_1}{M} \end{bmatrix} \tag{17}$$

where $M = M_1 + M_2 + M_3 + M_4 + M_5$. Note that the disturbances are assumed to be measurable and bounded by $|w_1| \le \Delta_1$ and $|w_2| \le \Delta_2$, where Δ_1 and Δ_2 may depend on x.

The design goal for the nonlinear optimal controller is to find a feedback control $u(x)$ that stabilizes system given in Eq. (14) while minimizing the cost functional[18,19]

$$J = \int_0^\infty [l(x) + u^T r(x) u]\,\mathrm{d}t \tag{18}$$

with $l(x) \ge 0$ and $r(x) > 0$ for all x. If there exists $V(x) \ge 0$ that satisfies the Hamilton–Jacobi–Isaacs (HJI) equation associated with the system given by Eq. (14) and the cost of Eq. (18),

$$\inf_u \sup_w \left[l(x) + u^T r(x) u + L_f V(x) + L_g V(x) u + \sum_{k=1}^{2} L_{d_k} V(x) w_k \right] = 0 \tag{19}$$

where $L_f V(x)$, $L_g V(x)$, and $L_{d_k} V(x)$ denote the Lie derivatives of $V(x)$ with respect to $f(x)$, $g(x, w)$, and d_k, respectively (see Ref. 20). Then the nonlinear optimal control law can be expressed in the following form:

$$u = -\tfrac{1}{2} r^{-1}(x)[L_g V(x)]^T \tag{20}$$

where $V(x)$ is the optimal value function of J. However, it is extremely difficult or may not be feasible to solve the HJI equation to find the solution $V(x)$ in a direct nonlinear optimal control design. Therefore, the inverse nonlinear optimal control design is adopted. In the inverse nonlinear optimal control approach, a stabilizing feedback control law is designed first and then shown to be optimal with respect to a well-defined cost functional of the form of Eq. (18). In other words, the functions $l(x)$ and $r(x)$ are a posteriori determined by the chosen stabilizing feedback control law, rather than a priori specified by the designer.[21,22]

One way to stabilize the nonlinear system is to select a Lyapunov function $V(x)$ and then find a feedback control $u(x)$ that renders $\dot{V}(x, u)$ negative definite. However, with an arbitrary choice of $V(x)$, this attempt may fail. Therefore, in this study, a stabilizing control law is formulated based on robust control Lyapunov function (RCLF) (see Refs. 23 and 24). For the nonlinear system given in Eq. (14), $V(x)$ is an RCLF if, for all $x \ne 0$,

$$L_g V(x) = 0 \Rightarrow L_f V(x) + \sum_{k=1}^{2} \left| L_{d_k} V(x) \right| \Delta_k < 0 \tag{21}$$

Note that the classic Lyapunov function only allows us to assess the stability of the closed-loop system generated by a predetermined feedback control, but RCLF allows us to assess the stability of a system without predetermined feedback control.

A stabilizing nonlinear optimal control law $u_p(x)$ that renders the RCLF $V(x)$ an optimal value function is proposed in this study, based on Sontag's[25] formula (also see Ref. 26) as follows:

$$u_p = -p(x)[L_g V(x)]^T \tag{22}$$

with

$$p(x) = \begin{cases} \dfrac{\Psi(x) + \sqrt{\{\Psi(x)\}^2 + \left\{[L_g V(x)][L_g V(x)]^T\right\}^2}}{[L_g V(x)][L_g V(x)]^T}, & \text{if} \quad L_g V(x) \neq 0 \\ 0, & \text{if} \quad L_g V(x) = 0 \end{cases} \tag{23}$$

where

$$\Psi(x) = L_f V(x) + \sum_{k=1}^{2} \left| L_{d_k} V(x) \right| \Delta_k \tag{24}$$

When $r_p^{-1}(x) = 2p(x)I$ is defined, the control law given by Eq. (22) takes the form

$$u_p = -\tfrac{1}{2} r_p^{-1}(x)(L_g V(x))^T \tag{25}$$

and the negative definite of $\dot{V}(x)$ is achieved with the control $u^* = -\frac{1}{2}u_p(x)$ for all $x \neq 0$, that is,

$$\begin{aligned} \sup_w \dot{V}(x)|_{u^*} &= \Psi(x) - \tfrac{1}{2} p(x) L_g V(x)[L_g V(x)]^T \\ &= -l_p(x) < 0 \end{aligned} \tag{26}$$

Then, $V(x)$ is a solution of the HJI equation

$$l_p(x) + \Psi(x) - \tfrac{1}{4}[L_g V(x)]\, r_p^{-1}[L_g V(x)]^T = 0 \tag{27}$$

Therefore, it is shown that the control law is optimal for the cost functional of the form

$$J = \int_0^\infty [l_p(x) + u^T r_p(x) u]\, \mathrm{d}t \tag{28}$$

For the system given by Eq. (14), the following function is chosen as an RCLF in this study:

$$V(x) = \tfrac{1}{2}x_1^2 + \tfrac{1}{2}(x_1 + x_2)^2 \tag{29}$$

The necessary controller takes the form of Eq. (25) where

$$\begin{aligned} L_f V(x) &= 2x_1 x_2 + x_2^2 + (x_1 + x_2)[-(K_1/M)x_1 - (C_1/M)x_2] \\ L_g V(x) &= -(x_1 + x_2)\tanh\{[(x_2 - w_2) + \lambda_1(x_1 - w_1)]\lambda_2\}/M \\ L_{d_1} V(x) &= (x_1 + x_2)(K_1/M), \qquad L_{d_2} V(x) = (x_1 + x_2)(C_1/M) \\ \Delta_1 &= 3|x_1| + 3|x_2|, \qquad \Delta_2 = 3|x_1| + 3|x_2| \end{aligned} \tag{30}$$

However, because the control $u(x)$ given by Eq. (14) is the magnitude of the MR yield force, the feasible control $u_p(x)$ to apply to the MR seat suspension should be bounded by $u_p \geq 0$. This physically means that the MR seat suspension is a semi-active actuation system.

Injury Assessment Criteria

To evaluate the protection for injury of occupants in the helicopter due to the crash landing, the injury assessment criteria for each part of the human body for axial loading are reviewed. However, because most of the injury criteria for helicopter crashing are not available in the public literature, the injury assessment is performed with the injury criteria for car crashing established by the automotive industry. Note that the injury assessment criteria reference values show variability in nature because human beings are widely varied and large number of possible injuries are highly situation dependent.

Criteria for Pelvis

The Federal Motor Vehicle Safety Standard (FMVSS) 208 on frontal impact assessment criteria proposed lower extremity injury criteria to limit the axial loads in the femur for the adult dummies: 10 kN for 50th percentile male and 6.8 kN for the 5th percentile female. Morgan et al.[27] suggested that the femur force was a very good predictor of pelvic injury and that a femur force of 10 kN corresponded to a 35% probability of fracture. According to the assessment protocol developed by the European New Car Assessment Programme (EuroNCAP), the femur compression force at higher performance protection must be less than 3.8 kN for 5% risk of pelvic injury and, at lower protection performance, be less than 7.56 kN for 10 ms (Ref. 28), which is the same as the femur fracture limit of the European Enhanced Vehicle Safety Committee (EEVC). On the other hand, FMVSS 214[29] on side impact assessment criteria proposed that the pelvis acceleration must not exceed a 130-g limit and the EEVC suggested that pubic symphysis force in the pelvic region must be less than 6.0 kN. As addressed in the cited standards, there are no consistent pelvic injuries for axial loading. However, from these standards, we deduce that the pelvis force ranging from 3.8 to 10 kN may cause the injuries in the pelvic region. Therefore, we use the lower force value of 3.8 kN as moderate pelvic injury assessment criterion and the higher force value of 10 kN as severe pelvic injury assessment criterion in this study.

Criteria for Upper Torso

The upper torso includes the thorax and the spine. Because only vertical motion is considered in this study, injuries may occur in the spine. The spine consists of three parts: cervical, thoracic, and lumbar vertebras. The cervical vertebras correspond to the top part of the spine and are connected to the head. The thoracic vertebras correspond to the middle part of the spine and the lumbar vertebras to the lower part of the spine. The lumbar vertebras are connected to the pelvis. In terms of load-bearing function, the cervical and lumbar vertebras are important. Because the lumbar vertebras are linked to the pelvis, the upper torso injury criterion is chosen based on estimating the injury of the cervical vertebras. The EuroNCAP protocol proposed the maximum cervical tension force must be less than 2.7 kN in higher protection performance. In lower protection performance, the maximum cervical tension force must be less 3.3 kN; this is the same as the limit of the EEVC. Yoganandan et al.[30] reported that the injury of the cervical vertebras happened at the tension force of 1.6 kN. On the other hand, Maiman et al.[31] suggested that the compression force for the cervical injury is about twice greater than the tension force and that the maximum compression force is 7.4 kN. According to the FMVSS 208, the tension force for the cervical injury must be less than 4.17 kN and the compression force must be less than 4.0 kN. Because the force limit varies for compression and tension motion, the injury criteria for the cervical vertebras are determined for both compression and tension. Therefore, in this study, the moderate and severe cervical vertebras injury criteria for compression are chosen to be 4.0 and 7.4 kN, respectively. In addition, the moderate and severe cervical vertebras injury criteria in tension are chosen to be 1.6 and 3.3 kN, respectively.

Criteria for Viscera

The abdomen includes two main types of organs, that is, the solid and the hollow organs, which behave quite differently under the various types of mechanical loading. The solid organs include

the liver, spleen, pancreas, kidneys, adrenal glands, and ovaries; the hollow organs include the stomach, small and large intestines, urinary bladder, and the uterus.[14,32] Therefore, the protection of the abdomen is critically important, and its injury criterion is defined by total abdominal force. The EuroNCap protocol proposed that, at higher protection limit, total abdominal force is limited to 1.0 kN and that, at lower protection limit, it is 2.5 kN. The total abdominal force of 2.5 kN is also the EEVC limit. Therefore, moderate and severe viscera injury criteria are chosen to be 1.0 and 2.5 kN, respectively.

Criteria for Head

The head injury is evaluated mainly on the basis of head injury criterion (HIC) with a 15-ms limit on the period over which it is calculated, that is,

$$\mathrm{HIC}_{15} = \max\left\{(t_2 - t_1)\left[\frac{1}{t_2 - t_1}\int_{t_1}^{t_2} a(t)\,\mathrm{d}t\right]^{2.5}\right\} \tag{31}$$

where t_1 is the initial time of integration, t_2 is the final time of integration, and $a(t)$ is the resultant acceleration in gravitational acceleration measured at the center-of-gravity of the head. The FMVSS 208 established that the maximum value of 700 for the HIC_{15} is estimated to represent a 5% risk of a severe head injury and that a value of 1000 for the HIC_{15} corresponds to a 16% risk of serious brain injury.[33] Therefore, in this study, the maximum value of 700 is chosen for the moderate injury criterion for the head and the value of 1000 is the severe injury criterion for the head. Note that severe head injury refers to 1) skull fracture with leak of cerebrospinal fluid, 2) laceration of cerebellum or cerebrum, 3) hematoma (epidural, subdural, intracerebral, or intracerebellar) and 4) unconsciousness between 1 and 24 h (Ref. 14).

Simulation Results

The performances of the seat suspensions are assessed for three cases: 1) passive hydraulic seat suspension, 2) passive MR seat suspension when the magnetic field and, hence, the yield stress are held constant, and 3) semi-active MR seat suspension when the magnetic field in the MR damper is controlled using the nonlinear optimal feedback control algorithm.

Sinusoidal Vibration

The helicopter produces cyclic and constant vibration during flight, and the vibration is believed to reduce occupant ride comfort and increase physical fatigue, and, furthermore, induce chronic low back pain.[34] Therefore, we first evaluate biodynamic response mitigation of the MR seat suspension to sinusoidal vibration to assess its vibration attenuation performance in the frequency domain.

In this case of sinusoidal vibration, the initial vertical velocity is assumed to be zero and the floor undergoes sinusoidal excitation. The sinusoidal excitation has a constant displacement amplitude of 25.4-mm (1-in.) peak, and because most interesting frequencies in seat suspensions fall below 20 Hz, the frequency of excitation is swept through the frequency range of 0.5–20 Hz. To emulate the practical situation of control action, control input $u_p(x)$ is assumed to pass through a first-order low-pass filter given by

$$\dot{u}_{pf} = (u_p - u_{pf})/\tau \tag{32}$$

where u_{pf} is the filtered control input and τ is the time constant, that is, $\tau = 10$ ms in this study. Because it neglects high-order dynamics of the control input, the filter control input u_{pf} has time-delay-like practical actuators. The filtered control input u_{pf} is incorporated with the governing equations (1–5) to calculate the biodynamic responses of the MR seat suspension. In addition, to consider practical yield stress characteristics of MR fluids, the magnitude of yield force F_0 is assumed to be saturated at a maximum value of 1.5 kN. On the other hand, the assessment of the MR seat suspension is performed on the basis of transmissibility calculated from the ratio of rms acceleration of each part of the human body to rms acceleration excitation. In addition the vibration attenuation performance of the MR seat suspension is compared to that of a seat suspension using a passive hydraulic damper. However, parameters of passive hydraulic seat suspensions for helicopters are not reported in the literature; parameters such as stiffness and damping coefficient for the passive hydraulic seat suspension are chosen on the basis of an existing passive hydraulic seat suspension for an off-road vehicle.[35] In this study, the stiffness and damping of the passive hydraulic seat suspension are chosen to be 22.6 kN/m and 1100 N · s/m.

Figure 3 shows the simulated transmissibilities of each part of the human body to a sinusoidal excitation load. The thick solid line indicates the response of the semi-active MR seat suspension using the nonlinear optimal control algorithm and thin solid line the passive MR seat suspension with a constant yield force of 1.5 kN. The dashed line is for the response of the passive hydraulic seat suspension. As seen in Fig. 3, the passive MR seat suspension shows better vibration attenuation performance below the first resonance frequency of around 2 Hz than the passive hydraulic seat suspension.

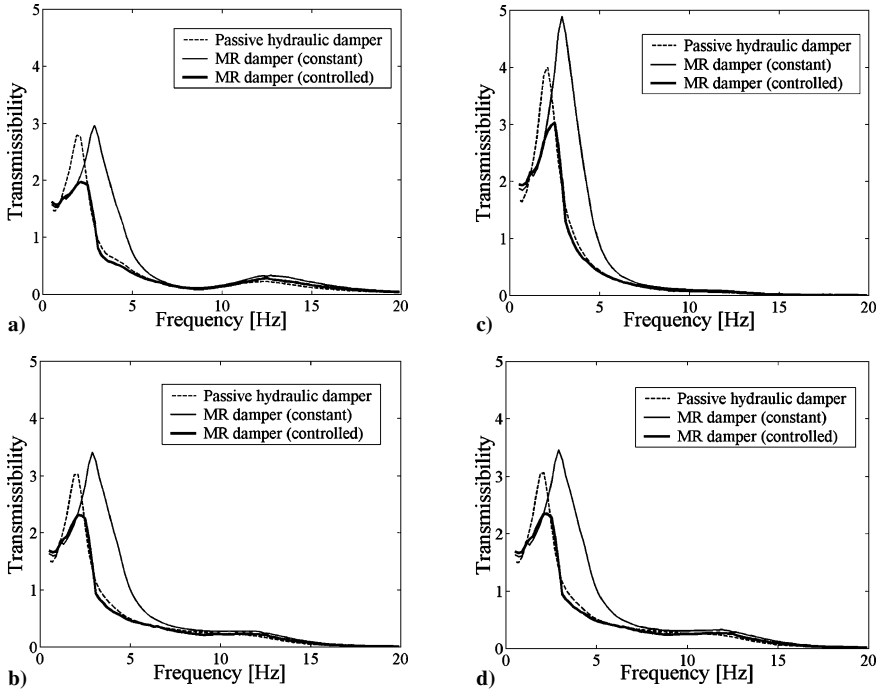

Fig. 3 Simulated transmissibilities of each part of human body on MR seat suspension: a) pelvis, b) upper torso, c) viscera, and d) head.

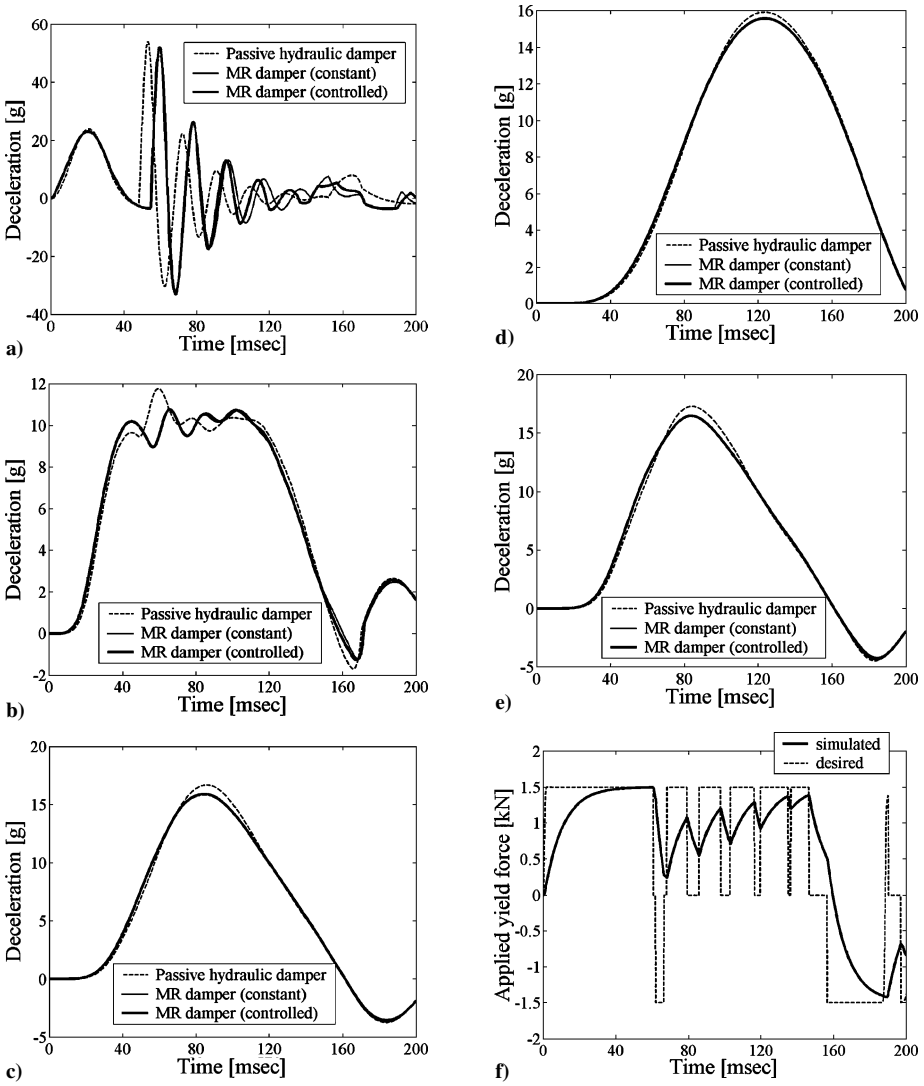

Fig. 4 Simulated biodynamic time responses of MR seat suspension system to shock load: a) deceleration of seat, b) deceleration of pelvis, c) deceleration of upper torso, d) deceleration of viscera, e) deceleration of head, and f) applied yield force.

However, in the frequency range of 4–8 Hz, which is closely associated with occupants' ride comfort,[36,37] the passive MR seat suspension is much worse than the passive hydraulic seat suspension. However, the semi-active MR seat suspension shows better vibration attenuation performance over most of the simulated frequency range when compared to the passive hydraulic and passive MR seat suspensions.

Shock Load

During a crash or high sink rate landing, the floor of the helicopter undergoes a shock deceleration, and the magnitude of the shock is dependent on its duration time and the initial vertical landing velocity of the helicopter as shown in Eq. (8). The larger the initial landing velocity, the greater the shock deceleration is produced. Also, the shorter the duration time, the greater the shock deceleration is produced. In practice, the duration of shock load due to a crash or high sink rate landing varies with respect to materials and mechanisms of the airframe and the existence of energy-absorbing devices such as landing gears. Therefore, in this study, it is assumed that the shock load, which is first reduced by airframe or landing gears, is applied to the floor and its duration ($t_s = 30$ ms) is determined as similar to shock test data measured.[17,38,39]

Figure 4 shows the simulated biodynamic time responses of the MR seat suspension to the shock load due to a crash landing. In this case, the initial vertical landing velocity of the helicopter is 6.71 m/s (22 ft/s) and a half-sine shock load is developed during 0–30 ms. As shown in Fig. 4a, because of the bottoming out of the seat suspension due to the stroke limit of the damper, the peak deceleration of the seat occurs around 60 ms after impact. The magnitudes of the peak deceleration of the passive and semi-active MR seat suspensions are not only more reduced than those of the passive hydraulic seat suspension, but also the peak deceleration time is delayed 6.4 ms beyond that for the passive hydraulic seat suspension. Because the pelvis is in direct contact with the seat cushion, the area of the deceleration for the pelvis is closer to the shape of a square. The start time of the shock deceleration on the upper torso is later than that of the pelvis. It arises from the fact that the shock deceleration is transmitted from the floor to the human body. As observed in Fig. 4, the maximum peak deceleration of each part on the semi-active MR seat suspension is smaller than that of the passive hydraulic seat suspension. However, in the case of shock load, the passive MR seat suspension also shows as good a shock attenuation performance as the semi-active MR seat suspension. The applied yield force F_y under the control algorithm is shown in Fig. 4f. The solid line indicates the simulated yield force and the dashed line the desired yield force. In practical situations, the applied yield force develops fully after a time delay.

Figure 5 shows the simulated biodynamic responses of the MR seat suspension with respect to initial vertical landing velocity. In this case, the initial vertical crash landing velocity varies from 6.1 to 12.2 m/s (20 to 40 ft/s) (Refs. 15, 35, and 36). For the pelvis, the upper torso, and the viscera, their peak forces determined by (each mass) multiplied by (maximum magnitude of deceleration) are presented to assess crew injuries. For the head, HIC_{15} calculated

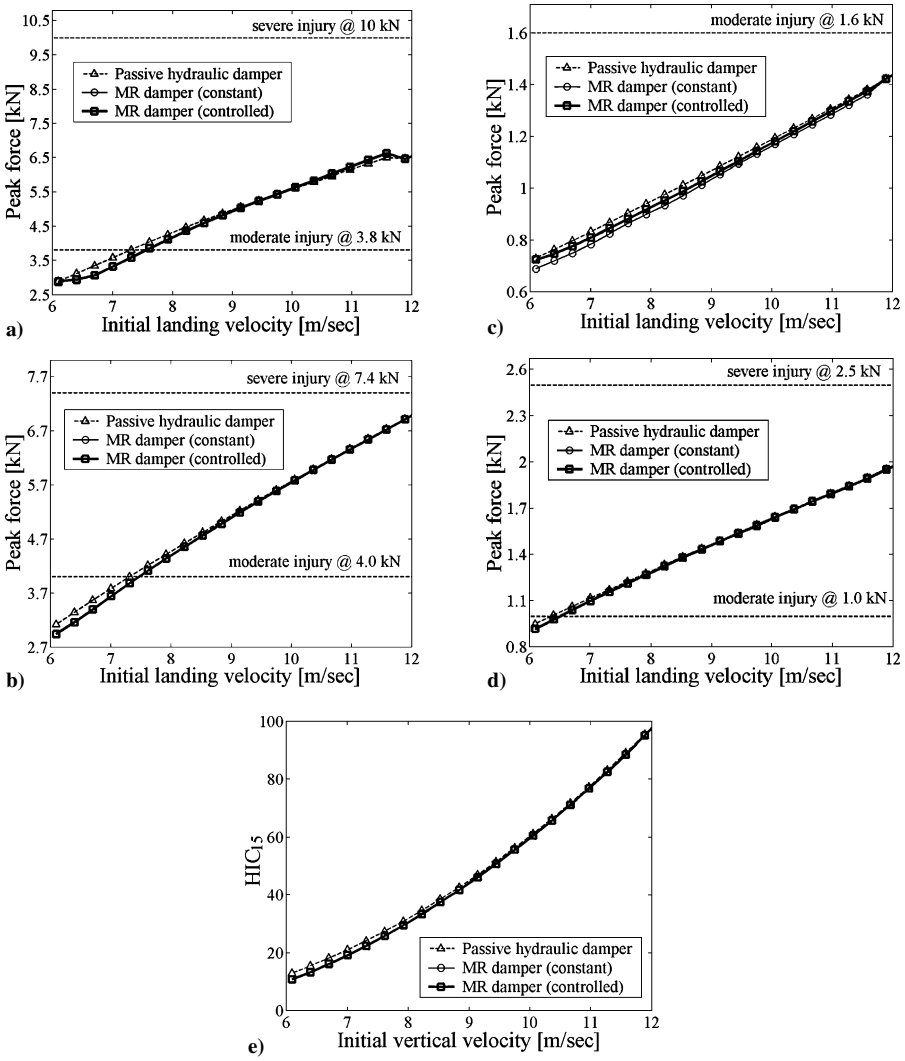

Fig. 5 Simulated biodynamic responses of MR seat suspension with respect to initial vertical landing velocity: a) pelvis, b) upper torso in compression, c) upper torso in tension (severe injury threshold, 3.3 kN), d) viscera, and e) head (moderate injury threshold, 700; severe injury threshold, 1000).

from the simulated deceleration response of the head is presented. Because the assessment of the upper torso injury is evaluated based on injuries of the cervical vertebras for both compression and tension, the compression and tension peak forces of the upper torso are determined by considering the sign of the relative displacement between the head and upper torso, $z_5 - z_3$. If $(z_5 - z_3) \geq 0$, the cervical vertebras are in a compression state and vice versa.

For the pelvis, the moderate and severe injury criteria were chosen to be 3.8 and 10 kN, respectively, in this study. In both cases of the passive and semi-active MR seat suspensions, the moderate pelvis injury does not occur below the initial vertical landing velocity of about 7.8 m/s, and the severe pelvic injury does not occur at these simulated crash landing velocities, as shown in Fig. 5a. On the other hand, the passive hydraulic suspension system does not present severe pelvic injury, but moderate injury may occur above a sink rate of about 7.3 m/s.

The moderate and severe injury criteria for the cervical vertebras in compression were chosen to be 4.0 and 7.4 kN, respectively. In both cases of the passive and semi-active MR seat suspensions, the moderate injury in compression does not occur below the crash landing velocity of about 7.6 m/s, and the severe injury does not occur at all, as shown in Fig. 5b. In tension mode, the moderate and severe injury criteria for cervical vertebras were chosen to be 1.6 and 3.3 kN, respectively. As observed in Fig. 5c, the tension peak forces of the upper torso on three seat suspensions do not exceed the moderate injury threshold of 1.6 kN. Therefore, moderate and/or severe cervical vertebras injuries for the tension mode are not likely in this study. On the other hand, for the passive hydraulic seat suspension, the moderate cervical injury in compression does not occur below the crash landing velocity of about 7.3 m/s, and cervical vertebras injury in tension do not occur at simulated crash landing velocities.

For the viscera, the moderate and severe injury criteria were chosen by 1.0 and 2.5 kN, respectively. In both cases of the passive and semi-active MR seat suspensions, the moderate viscera injury starts to occur on 6.7 m/s, but the severe viscera injury threshold is not exceeded in the simulated crash landing velocities, as shown in Fig. 5d. For the passive hydraulic seat suspension, the moderate viscera injury threshold is 6.3 m/s. However the severe viscera injury is unlikely for these simulated crash landing velocities.

For the head, the maximum values of 700 and 1000 were chosen for the moderate and the severe injury criteria. As observed in Fig. 5e, HIC_{15} of all three seat suspensions fall below the maximum value of 100 for our simulated velocities, which is far below the moderate head injury criterion. Therefore, brain injury is quite unlikely in this study.

Overall, the passive and semi-active MR seat suspensions present better shock mitigation performance than the passive hydraulic seat suspension. In addition, in contrast to the sinusoidal excitation case, the MR seat suspension with constant yield force shows good shock attenuation performance similar to the MR seat suspension under the control algorithm.

Conclusions

The simulated biodynamic responses of an MR seat suspension to sinusoidal vibration, as well as shock loads due to a vertical crash landing of a helicopter, were presented. In doing so, an MR seat

suspension model was developed including body components such as pelvis, upper torso, viscera, and head. From the model, the governing equation of motion of the MR seat suspension considering the human body was derived. Based on this equation, a semi-active nonlinear optimal control algorithm appropriate for the MR seat suspension was proposed and formulated. The simulated control performance of the MR seat suspension was evaluated under both sinusoidal excitation and shock loads. In addition, the mitigation of injuries to humans due to such shock loads on the MR seat suspension was also evaluated and compared with those of a passive hydraulic seat suspension and a passive MR seat suspension. For the sinusoidal excitation case, it was observed that the semi-active MR seat suspension shows better vibration attenuation performance over the simulated frequency range than both the passive hydraulic or passive MR seat suspensions. It was also shown, for the shock load case, that both the passive and semi-active MR seat suspensions present better shock attenuation performance than the passive hydraulic seat suspension. A key conclusion is that vibration attenuation performance can be substantially improved using a semi-active MR seat suspension without sacrificing crashworthiness or increasing injury rates under crash landing conditions.

References

[1]Cheng, Z. Q., Pilkey, W. D., Balandin, D., Bolotnik, N. N., Crandall, J. R., and Shaw, C. G., "Optimal Control of Helicopter Seat Cushions for the Reduction of Spinal Injuries," *International Journal of Crashworthiness*, Vol. 6, No. 3, 2001, pp. 321–337.

[2]Balandin, D. V., Bolotnik, N. N., and Pilkey, W. D., "Computational Methods for a Limiting Performance Analysis," *Optimal Protection from Impact, Shock, and Vibration*, Gordon and Breach Science, Amsterdam, 2001, Chap. 8, pp. 255–345.

[3]Rakheja, S., Afework, Y., and Sankar, S., "An Analytical and Experimental Investigation of the Driver-Seat-Suspension System," *Vehicle System Dynamics*, Vol. 23, No. 3, 1994, pp. 501–524.

[4]Stein, G. J., "A Driver's Seat with Active Suspension of Electropneumatic Type," *Journal of Vibration and Acoustics*, Vol. 119, No. 2, 1997, pp. 230–235.

[5]Choi, Y. T., and Wereley, N. M., "Comparative Analysis of the Time Response of Electrorheological and Magnetorheological Dampers Using Nondimensional Parameters," *Journal of Intelligent Material Systems and Structures*, Vol. 13, No. 7/8, 2002, pp. 443–451.

[6]Wu, X., and Griffin, M. J., "A Semi-Active Control Policy to Reduce the Occurrence and Severity of End-stop Impacts in a Suspension Seat with an Electrorheological Fluid Damper," *Journal of Sound and Vibration*, Vol. 203, No. 5, 1997, pp. 781–793.

[7]Choi, S. B., Choi, J. H., Nam, M. H., Cheong, C. C., and Lee, H. G., "A Semi-Active Suspension Using ER Fluids for a Commercial Vehicle Seat," *Journal of Intelligent Material Systems and Structures*, Vol. 9, No. 8, 1999, pp. 601–606.

[8]Choi, S. B., Nam, M. H., and Lee, B. K., "Vibration Control of MR Seat Damper for Commercial Vehicles," *Journal of Intelligent Material Systems and Structures*, Vol. 11, No. 12, 2000, pp. 936–944.

[9]Park, C., and Jeon, D., "Semiactive Vibration Control of a Smart Seat with an MR Fluid Damper Considering its Time Delay," *Proceedings of the 8th International Conference on Electrorheological Fluids and Magnetorheological Suspensions*, World Scientific, Singapore, Republic of Singapore, 2001.

[10]McManus, S. J., St. Clair, K. A., Boileau, P. É., and Boutin, J., "Evaluation of Vibration and Shock Attenuation Performance of a Suspension Seat with a Semi-Active Magnetorheological Fluid Damper," *Journal of Sound and Vibration*, Vol. 253, No. 1, 2002, pp. 313–327.

[11]Gunston, T., and Griffin, M. J., "The Isolation Performance of a Suspension Seat over a Range of Vibration Magnitudes Tested with an Anthropodynamic Dummy and Human Subjects," *Inter-noise '99, Proceedings of 28th International Congress and Exposition on Noise Control Engineering*, Inst. of Noise Control Engineering, Saddle River, NJ, 1999, pp. 949–954.

[12]Balandin, D. V., Bolotnik, N. N., and Pilkey, W. D., "Limiting Performance Analysis of Impact Isolation Systems for Injury Prevention," *Shock and Vibration Digest*, Vol. 33, No. 6, 2001, pp. 453–472.

[13]Carden, H. D., "Effect of Crash Pulse Shape on Scat Stroke Requirements for Limiting Loads on Occupants of Aircraft," NASA TP 3126, Feb. 1992.

[14]Zong, Z., and Lam, K. Y., "Biodynamic Response of Shipboard Sitting Subject to Ship Shock," *Journal of Biomechanics*, Vol. 35, No. 1, 2002, pp. 35–43.

[15]Choi, Y. T., Wereley, N. M., and Jeon, Y. S., "Semi-Active Vibration Isolation Using Magnetorheological Isolators," *Journal of Aircraft* (to be published).

[16]Rebelle, J., "Development of a Numerical Model of Seat Suspension to Optimise the End-stop Buffers," *35th United Kingdom Group Meeting on Human Response to Vibration*, Univ. of Southampton, Southampton, England, U.K., 2000, pp. 221–238.

[17]Jackson, K. E., Fasanella, E., Boitnott, R., McEntire, J., and Lewis, A., "Occupant Response in a Full-scale Crash Test of the Sikorsky ACAP Helicopter," *Proceedings of 58th American Helicopter Society Annual Forum*, AHS International, Alexandria, VA, 2002, pp. 1922–1938.

[18]Sepulchre, R., Jankovic, M., and Kokotovic, P., "Stability Margins and Optimality," *Constructive Nonlinear Control*, Springer, London, 1997, Chap. 3.

[19]Shue, S. P., Sawan, M. E., and Rokhsaz, K., "Optimal Feedback Control of a Nonlinear System: Wing Rock Example," *Journal of Guidance, Control, and Dynamics*, Vol. 19, No. 1, 1996, pp. 166–171.

[20]Slotine, J. J., "Feedback Linearization," *Applied Nonlinear Control*, Prentice–Hall, London, 1991, Chap. 6, pp. 207–275.

[21]Kristic, M., and Li, Z. H., "Inverse Optimal Design of Input-to-State Stabilizing Nonlinear Controllers," *IEEE Transactions on Automatic Control*, Vol. 43, No. 3, 1998, pp. 336–350.

[22]El-Farra, N. H., and Christofides, P. D., "Robust Near-Optimal Output Feedback Control of Non-Linear Systems," *International Journal of Control*, Vol. 74, No. 2, 2001, pp. 133–157.

[23]Kokotovic, P., and Arcak, M., "Constructive Nonlinear Control: A Historical Perspective," *Automatica*, Vol. 37, No. 5, 2001, pp. 637–662.

[24]El-Farra, N. H., and Christofides, P. D., "Integrating Robustness, Optimality and Constraints in Control of Nonlinear Process," *Chemical Engineering Science*, Vol. 56, No. 5, 2001, pp. 1841–1868.

[25]Sontag, E. D., "A Universal Construction of Artstein's Theorem on Nonlinear Stabilization," *Systems and Control Letters*, Vol. 13, No. 2, 1989, pp. 117–123.

[26]Freeman, R. A., and Primbs, J. A., "Control Lyapunov Functions: New Ideas From an Old Source," *Proceedings of the 35th Conference on Decision and Control*, Univ. of Southampton, Southampton, England, U.K., 1996, pp. 3926–3931.

[27]Morgan, R., Eppinger, R. H., and Marcus, J., "Human Cadaver Patella–Femur–Pelvis Injury Due to Dynamic Frontal Impact to the Patella," *Proceedings of 12th International Conference on Experimental Safety Vehicles*, U.S. Dept. of Transportation, National Highway Safety Administration, Washington, DC, 1989.

[28]King, J. J., Fan, R. S., and Vargovick, R. J., "Femur Load Injury Criteria," 7th Stapp Car Crash Conf., Society of Automotive Engineers, SAE TP 730984, 1973.

[29]Samaha, R. R., Molino, L. N., and Maltese, M. R., "Comparative Performance Testing of Passenger Cars Relative to FMVSS 214 and the EU/96/EC/27 Side Impact Regulations: Phase I," *16th International Technical Conference on the Enhanced Safety of Vehicles*, Paper 98-S8-O-08, U.S. Dept. of Transportation, National Highway Safety Administration, Washington, DC, June 1998, pp. 1712–1759.

[30]Yoganandan, N., Pintar, F. A., Maiman, D. J., Cusick, J. F., Sances, A., and Walsh, P. R., "Human Head–Neck Biomechanics Under Axial Tension," *Medical Engineering and Physics*, Vol. 18, No. 4, 1996, pp. 289–294.

[31]Maiman, D. J., Sances, A., Myklebust, J. B., Larson, S. J., Houterman, C., Chilbert, M., and El-Ghatit, A. Z., "Compression Injuries of the Cervical Spine: A Biomechanical Analysis," *Neurosurgery*, Vol. 13, No. 3, 1983, pp. 254–260.

[32]Rouhana, S. W., "Biomechanics of Abdominal Trauma," *Accidental Injury: Biomechanics and Prevention*, edited by A. M. Nahum and J. W. Melvin, Springer-Verlag, New York, 1993, pp. 391–428.

[33]Mertz, H. J., Prasad, P., and Irwin, N. L., "Injury Risk Curves for Children and Adults in Frontal and Rear Collisions," 41st Stapp Car Crash Conf., Society of Automotive Engineers, SAE TP 973318, 1997.

[34]Oliveira, C. G., Simpson, D. M., and Nada, J., "Lumbar Back Muscle Activity of Helicopter Pilots and Whole-body Vibration," *Journal of Biomechanics*, Vol. 34, No. 10, 2000, pp. 1309–1315.

[35]Tewari, V. K., and Prasda, N., "Three-DOF Modelling of Tractor Seat-Operator System," *Journal of Terramechanics*, Vol. 36, No. 4, 1999, pp. 207–219.

[36]Griffin, M. J., "Vibration Discomfort," *Handbook of Human Vibration*, Academic Press, London, 1996, Chap. 3, pp. 43–122.

[37]Pavic, A., and Reynolds, P., "Vibration Serviceability of Long-Span Concrete Building Floors. Part 1: Review of Background Information," *Shock and Vibration Digest*, Vol. 34, No. 3, 2002, pp. 191–211.

[38]Fasanell, E. L., and Jackson, K. E., "Impact Testing and Simulation of a Crashworthy Composite Fuselage Section with Energy-Absorbing Seats and Dummies," *58th American Helicopter Society Annual Forum*, AHS International, Alexandria, VA, June 2002, pp. 1961–1972.

[39]Lyle, K. H., Jackson, E., and Fasanella, E. L., "Simulation of Aircraft Landing Gears with a Nonlinear Dynamic Finite Element Code," *Journal of Aircraft*, Vol. 39, No. 1, 2002, pp. 142–147.